A study of microstructure and mechanical property of a burn-resistant Ti alloy fabricated by HIPping

Ding, Rengen; Chu, Mingqiang; Zhang, Shuyan

DOI:
10.1016/j.matchar.2020.110280

Document Version
Peer reviewed version

Citation for published version (Harvard):
Ding, R, Chu, M & Zhang, S 2020, 'A study of microstructure and mechanical property of a burn-resistant Ti alloy fabricated by HIPping', *Materials Characterization*, vol. 163, 110280.
https://doi.org/10.1016/j.matchar.2020.110280

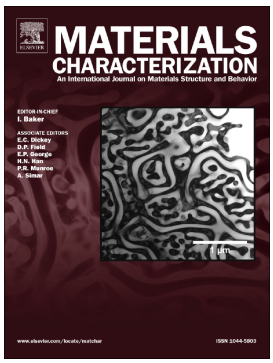

A study of microstructure and mechanical property of a burn-resistant Ti alloy fabricated by HIPping

Rengen Ding, Mingqiang Chu, Shuyan Zhang

PII: S1044-5803(20)30170-4

DOI: https://doi.org/10.1016/j.matchar.2020.110280

Reference: MTL 110280

To appear in: *Materials Characterization*

Received date: 18 January 2020

Revised date: 12 March 2020

Accepted date: 16 March 2020

Please cite this article as: R. Ding, M. Chu and S. Zhang, A study of microstructure and mechanical property of a burn-resistant Ti alloy fabricated by HIPping, *Materials Characterization* (2020), https://doi.org/10.1016/j.matchar.2020.110280

A study of microstructure and mechanical property of a burn-resistant Ti alloy fabricated by HIPping

Rengen Ding[1,2*], Mingqiang Chu[1], and Shuyan Zhang[1*]

1: Centre of Excellence for Advanced Materials, Dong Guan, Guang Dong, China
2: School of Metallurgy and Materials, University of Birmingham, Birmingham, B15 2TT, UK
**Correspondence authors: r.ding@bham.ac.uk; shuyan.zhang@ceamat.com*

Abstract

A burn-resistant Ti-25V-15Cr-2Al-0.2C alloy was fabricated by hot isostatic pressing (HIPping) from the prealloyed powders under a pressure of 200 MPa and at 900, 950, and 980°C for 2 h. Microstructure was examined using scanning electron microscope (SEM) equipped with electron backscatter diffraction (EBSD) detector and transmission electron microscope (TEM). Tensile tests were to evaluate mechanical behaviour of the HIPped samples. The results show that HIPping temperature clearly affects the microstructure of the HIPped samples, thus the mechanical properties. For example, lower HIPping temperature produced more porosities at triple-junctions and more large grains resulted from the original powders, thus lower ductility was observed in the sample HIPped at 900°C. However, the sample HIPped at 980°C generates the best tensile properties with over 20% ductility, which are even better than those of as-extruded Ti-25V-15Cr-2Al-0.2C alloy.

Keywords: HIPping; Microstructure; Tensile property; Burn-resistant Ti alloy

1. Introduction

Titanium alloys have widely used in areo-frames and aero-engines. However, the problem of 'titanium fire' restricts the further use of Ti alloys in areo-engines. Thus, in the past 30 year, it has led to the development of burn-resistant Ti alloys that will not burn under the pressure, temperature and air flow of areo-engines in different countries [1-10]. For example, in the USA, a Ti-35V-15Cr based burn-resistant Ti alloy (, which was designated Alloy C) was developed by Pratt & Whitney [3,4]. This alloy, which is non-burning up to 600°C, has very

attractive high temperature mechanical properties, particularly in creep resistance and strength, and excellent cold forming capabilities being similar to standard beta Ti alloys [5]. However, Zhang et al. [6] studied effect of alloying content on oxidation behavior of Alloy C and found that Ti-25V-15Cr alloy had the best oxidation resistance among the Ti-V-Cr burn-resistant alloys. To increase the cost-competitiveness of Ti-25V-15Cr alloy, Al was also added into the Ti-V-Cr system. It has been demonstrated that 2 wt % Al addition results in a good balance of room-temperature ductility, strength and high-temperature properties in combination with burn resistance [7-9] but the dependence of its tensile ductility on oxygen content. Further investigations [1,7] showed that carbon addition brings about the following advantages: 1) enhancing clearly the ductility of the alloys; 2) reducing the tendency of α precipitation, thus improving the stability of the alloy system. It has also been demonstrated that the optimized carbon content is 0.2 wt.% [1,7]. These studies were undertaken jointly by the IRC and Rolls-Royce in UK. The researchers in China developed Si-contained burn-resistant alloys such as Ti-40 (Ti-25V-15Cr-0.2Si wt. %) [10]. Among these three alloys, Ti-25V-15Cr-2Al-0.2C burn-resistant β Ti alloy is the cheapest and has the lowest density (5.1 g/cm^3).

However, as-cast plus as-extruded Ti-25V-15Cr-2Al-0.2C alloy showed somewhat scatter in ductility [11], which may be associated with the carbides aligned along the extrusion axis. This as-extruded alloy also showed coarse grains (i.e. 70-90 μm) and carbides (i.e. 5-15 μm) [1]. This means that the mechanical properties (e.g. strength and ductility) of Ti-25V-15Cr-2Al-0.2C alloy may be further improved via refinement of grain and carbide. Powder metallurgy, e.g. hot isostatic pressing (HIPping) has been demonstrated to be an alternative method to refine microstructure. However, many studies have proved that microstructure and mechanical properties of HIPped Ti alloys are controlled by HIPping conditions (e.g. HIPping temperature, pressure or dwell time) [11-14]. Zhang [11] did some work on the effect of HIPping temperature (i.e. 850-950°C) and pressure (i.e. 100 and 150 MPa) on the microstructure and mechanical behaviour of Ti-25V-15Cr-2Al-0.2C alloy. It was found that HIPping slightly improved strength but led to a large scatter of ductility. Microstructural examination showed that such scatter may be attributed to the presence of prior particle boundaries (PPBs) in the HIPped sample. However, such PPBs may be

alleviated via modifying HIPping parameters (e.g. temperature and pressure).

In this study, thus, we use higher HIPping pressure and temperature to fabricate Ti-25V-15Cr-2Al-0.2C alloy so as to achieve better mechanical performance. Strength and ductility of the HIPped samples were assessed via tensile tests. Microstructure of the as-HIPped and tensile tested samples was evaluated using electron microscopy. Variation in the mechanical behavior of the HIPped samples with the HIPping parameters was discussed in terms of microstructural evolution.

2. Experimental procedure

2.1 Materials

Plasma rotating electrode processed (PREP) Ti-25V-15Cr-2Al-0.2C (wt.%) powder with size range of 100~250 μm (Fig. 1) was supplied by StarMet. HIPping was carried out in an EPSI Lab facility using a pressure of 200 MPa for 2h at 900, 950 and 980°C, respectively.

2.1 Microstructural characterisation

Samples for metallography were prepared following a standard metallographic procedure. The samples for EBSD were finally polished using 0.05 μm colloidal silica suspension. Microstructural examination was carried out in a FEI Quanta 3D scanning electron microscope. Grain size was measured using Oxford Instruments Nordlys EBSD detector with a step size of 2 μm. The ϕ3 mm discs for transmission electron microscopy (TEM) were cut from the as-HIPped sample or sectioned perpendicularly from the gauge length of the tensile failed samples, and then ground mechanically to 150 μm in thickness, electropolished in a solution of 5% perchloric acid, 35% butanol and 60% methanol at 25V and 243K using a twin-jet electropolisher. TEM examination was performed using a FEI Talos F200X microscope operating at 200 kV and equipped with Super-X energy dispersive X-ray spectroscope (EDS).

2.3 Tensile test

Tensile samples of 5 mm in diameter and 25.3 mm gauge length were machined from larger cylindrical samples so that the surface was removed. Three tensile tests for each condition were performed on a Zwick 1484 mechanical testing machine at a nominal strain rate of 5×10^{-4}/s at room temperature in air.

3. Results and discussion

3.1 Microstructure of as-HIPped samples

Figures 2 and 3 exhibit SEM images from the samples HIPped at 900, 950 and 980°C. Some large grains were found randomly in all three samples (Figs. 2 and 3), which may result from the original particles. The prior particle boundaries are still visible in the samples HIPped at 900°C and 950°C. Some porosities were found at triple-junctions of the sample HIPped at 900°C (Fig. 2b), which indicates that bonding of particles at 900°C for 2 h under a pressure of 200 MPa is not complete. Both factors (i.e. PPBs and porosities) could degrade the ductility of the HIPped samples. EBSD maps show clearly a bimodal distribution of grains and reveal PPBs in all three samples but more in the sample HIPped at 900°C (Figs. 4). Average grain size (the grains of >100 μm were not counted because they are assumed to result from powders) is 19.9±13.1 μm, 19.58±13.0 μm, and 21.85±14.76 μm for the samples HIPped at 900, 950 and 980°C, respectively. This shows that HIPping at 980°C promotes slightly grain growth but the number of large grain (i.e. >100 μm) decreases (Fig. 4). Extensive precipitates were observed in all three HIPped samples and the size of precipitates at grain boundaries is larger than those in the grain interiors (Fig. 5). Figure 5b is a scanning transmission electron microscopy (STEM) image obtained from the sample HIPped at 950°C and shows that the size of precipitates is from 200 nm up to 2 μm. Spot EDS shows that the precipitate is Ti-rich carbide (Fig. 6a). Selected area electron diffraction (SAED) patterns taken from a precipitate along different zone axes are shown in Figs. 6c-e. The analysis of diffraction combined with the profiles of EDS linescan indicates that the precipitate is an ordered fcc structure Ti_2C carbide with lattice parameter a = 0.43 nm. Such ordered Ti_2C-type carbide has been reported in Nb-Ti-C alloy [15] and the other Ti based alloys [16-18].

3.2 Tensile properties

Typical true stress-strain curves for the samples HIPped at each temperature are illustrated in figure 7, showing that the HIPping temperature does not influence clearly YS and work-hardening but the ductility increases with the HIPping temperature, thus increasing UTS (Table 1). A summary of tensile properties for the different HIPped samples combined with data from literature is given in Table 1 and it is clear from this data that either YS or UTS in this study were higher than literature data from either the HIPped or as-extruded samples. The HIPped Ti25V15Cr2Al0.2C alloy has higher YS than the as-extruded samples, which could be attributed to the following factors: 1) the HIPped alloy has fine grain size (~ 20 μm vs. ~ 70-90 μm for the as-extruded sample [1]); 2) HIPping produced finer carbides (0.2-2 μm vs. ~ 5-15 μm for the as-extruded alloy [1]). The influence of grain size on the YS of β Ti alloys could be described using the Hall-Petch equation [20, 21]:

$$\sigma_y = \sigma_0 + kd^{-1/2}$$

where σ_y is the flow stress at 0.2% strain, d is the average grain diameter, and σ_0 and k are constants. Using k = 0.73 MPa $m^{1/2}$ obtained from a β Ti alloy [22] to estimate the effect of grain refinement, the increasement of YS is 77 MPa when the grain size is reduced from 80 μm (, which is the mean value of the as-extruded sample) to 20 μm for this study. This value is slightly less than the experimental value of ~100 MPa (1028 MPa for this study vs. 924 MPa for the as-extruded sample) (Table 1). This discrepancy is because the contribution of the refiner carbides to strength is not involved.

By comparison between this study and Zhang's work, it could conclude that the higher pressure improves likely the strength of HIPped samples. Table 1 also shows that in this study HIPping temperature does not influence YS but the ductility increases with HIPping temperature. The samples HIPped at 980°C showed over 20% ductility for all three tensile tests and the best tensile properties for Ti25V15Cr2Al0.2C alloy, even better than the forged burn-resistant Ti-V-Cr-Si alloys (Table 1). Xu et al. [23] investigated that the HIPping temperature (i.e. 800-940°C) and pressure (i.e. 40-120 MPa) influenced the microstructure and mechanical properties of HIPped Ti6Al4V alloy, and found that higher temperature (900-940°C) and higher pressure (over 100 MPa) produced better mechanical properties.

3.3 Fractography and fracture mechanism

To better clarify the failure mechanisms of the HIPped samples and a large scatter in ductility for the samples HIPped at 900 and 950°C, the fracture surfaces of all three types of samples are carefully analysed. Overview of the fracture surfaces is showed in Fig. 8, illustrating a variety of fracture surface appearance with HIPping temperature. For example, the sample HIPped at 900°C showed intergranular failure with two types of grains (Figs. 8a1 and 8a2). The size of large intergranular facets is similar to the size of powders, which indicates that those intergranular facets could be caused by prior powders. Closer examination shows that either large (Fig. 8a2) or small (Fig. 8a3) intergranular surfaces consist of dimples but these dimples are shallow and underdeveloped in the large intergranular surfaces (not shown here). The dimples could be formed via voids nucleation at the carbide (Fig. 8a4). In the samples HIPped at 950°C and 980°C, although the fracture morphology of prior powder (e.g. arrowed in Fig. 8b2) is still observed, the number of such fracture features significantly decreases compared to the sample HIPped at 900°C. Thus, higher ductility is achieved in the samples HIPped at 950°C and 980°C (Table 1). However, a tensile sample HIPped at 950°C only has 14% ductility. After careful examination on its fracture surface, a crack initiation site (arrowed in Fig. 9a) was found, being from an uncompleted bonding region. Low UTS (1096 MPa) and ductility (i.e. 16%) were observed in a tensile sample HIPped at 900°C where the crack initiation site located likely at a triple-junction (Fig. 9d), which results probably from a porosity as observed in the polished sample (Fig. 2b). It should be mentioned here that such defect (porosity) was not found in the other tensile tested samples with good ductility. To further confirm fracture (intergranular) mode for all HIPped samples, observation of the longitudinal section of the fractured samples was also performed, showing that the failure is really related to the grain boundaries (Figs. 10a-c). Intergranular failure could be attributed to the following reasons: the brittle carbides were not able to accommodate too much deformation thus leading to cracking (black arrows in Figs. 8a4 and 10d), and the cracks could further propagate along grain boundary via linking of ruptured carbides or voids generated by decohesion of carbides with grain boundary. TEM examination also demonstrated that, although the carbide appears somewhat ductility which is proved by some

dislocations within the carbide (Fig. 11a), the carbide has a brittle character [24] and could not accommodate too much strain, thus leading to cracking (Fig. 11a). A TEM image taken from a tensile tested sample is illustrated in Fig. 11b, which shows that the sample is deformed predominantly via dislocation slip and that dislocations piled up at carbide/matrix interface (Fig. 11b). Further tension produces more dislocations, thus causing accumulated strain/stress at the carbide/matrix interface. Unfortunately, the character of Ti_2C carbide is brittle [24] and has low carbide/matrix interface strength [25], which inevitably leads to microcracking at the carbide/matrix interface (Fig. 11c). Thus, dimples which could produce via voids nucleation at carbide, were observed on fracture surfaces (Fig. 8).

Conclusions

Microstructure and tensile properties of the samples HIPped at different temperatures have been investigated using SEM, EBSD, TEM and tensile testing. The following conclusions can be drawn.

1. Some porosities were found at triple-junctions of the HIPped sample at 900°C, which leads to low ductility.
2. Large grains with the size being similar to powder were observed in all three HIPped samples but the number of large grains decreases with increasing HIPping temperature.
3. The carbide is an ordered fcc structure Ti_2C, the size of the carbide at grain boundary is larger than that within grain.
4. HIPping at 980°C produces the best tensile properties with over 20% ductility, which is associated with lower fraction of intergranular failure.

Acknowledgement

This work has been carried out with the financial support by the Program for Guangdong Introducing Innovative and Enterpreneurial Teams (No. 2016ZT06G025) and Guangdong Natural Science Foundation (No. 2017B030306014), China.

Data availability

The data that support the findings of this study is available from the corresponding authors on request.

References:

1. Y.G. Li, M.H. Loretto, D. Rugg, and W. Voice, Acta Mater., 49 (2001), 3011-3017.
2. Y.Q. Zhao, K.Y. Zhu, H.L. Qu, H. Wu, and X.M. Zhao, Mater. Sci. & Tech., 16 (2000), 1073-1075.
3. UK patent Application 2, 238, 057, 1987.
4. J.G. Hansen, D. Novotnak, M.F. Welter and J.R. Wood, in Ti'95: Science and Technology, Proceedings of the 8th World Conference on Titanium, ed. P.A. Blenkinsop, E.J. Efans and H.M. Flower. Institute of Materials, London, 1995, 675.
5. Z.Q. Chen,D. Hu, M.H. Loretto and X. Wu, Mater. Sci. & Tech., 20 (2004), 343.
6. X.D. Zhang, P.A. Blenkinsop, and N.A. Walker, in Ti'95: Science and Technology, ed. P.A. Blenkinsop, E.J. Efans and H.M. Flower. Institute of Materials, London, 1995, 2111.
7. Y.G. Li, P.A. Blenkinsop, M.H. Loretto, and N.A. Walker, Acta Mater., 46 (1998), 5777.
8. Y.G. Li, M.H. Loretto, P.A. Blenkinsop, W. Voice, D. Rugg, and N.A. Walker, paper present at the 3rd Rolls-Royce/AVIC Symposium on Advanced Engine Technology, Tianjin, China, 11-12 April 2000.
9. Y.G. Li, P.A. Blenkinsop, M.H. Loretto, D. Rugg, and W. Voice, Acta Mater., 47 (1999), 2889.
10. Y. Zhao, L. Zhou, K. Zhu, H. Qu, and H. Wu, Mater. Sci. and Tech., 17 (2001), 677.
11. K. Zhang, Ph.D. Thesis, University of Birmingham, 2010.
12. K. Zhang, J. Mei, N. Wain, and X. Wu, Metall. Mater. Trans. A 41(2010), 1033–1045.
13. L. Xu, R.P. Guo, C.G. Bai, J.F. Lei, R. Yang, J. Mater. Sci. Technol., 30(2014), 1289–1295.
14. D.P. Delo, H.R. Piehler, Acta Mater. 47(1999), 2841–2852.
15. R. Ding, H. Jiao, and I.P. Jones, Mater. Sci. & Eng. A, 483-484 (2008), 199.
16. P. Wanjara, R.A.L. Drew, J. Root, and S. Yue, Acta Mater., 48 (2000), 1443.
17. H. Goretzki, Physica status solid, 20 (1967), K141.

18. Z.Q. Chen, D. Hu, M.H. Loretto, X. Wu, Mater. Sci. Tech., 20 (2004), 343.
19. S. Xin, Y. Zhao, W. Zeng, H. Wu, and X. Mao, Ti-2007 Science and Technology, ed. M. Ninomi, S. Akiyama, M. Ikeda, M. Hagiwara, K. Maruyama, The Japan Institute of Metals (2007), 813.
20. E.O. Hall, Proc. Phys. Soc., London Ser. B, B64 (1951), 747-754.
21. N.J. Petch, J. Iron Steel Inst., 174 (1953), 25-31.
22. A. Bhattacharjee, P. Ghosal, A.K. Gogia, S. Bhargava, S.V. Kamat., Mater. Sci. and Eng. A, 452-453 (2007), 219-227.
23. L. Xu, R. Guo, C. Bai, J. Lei, and R. Yang, J. Mater. Sci. Tench., 30 (2014), 1289.
24. R. Ding and I.P. Jones, Mater. Sci. and Tech., 26 (2010), 323.
25. J. Lason, Metall. Trans. A, 7 (1976), 1497.

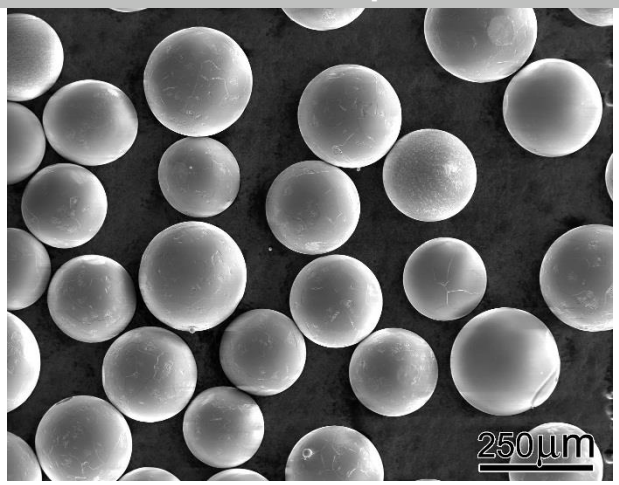

Figure 1 SEM image of powders

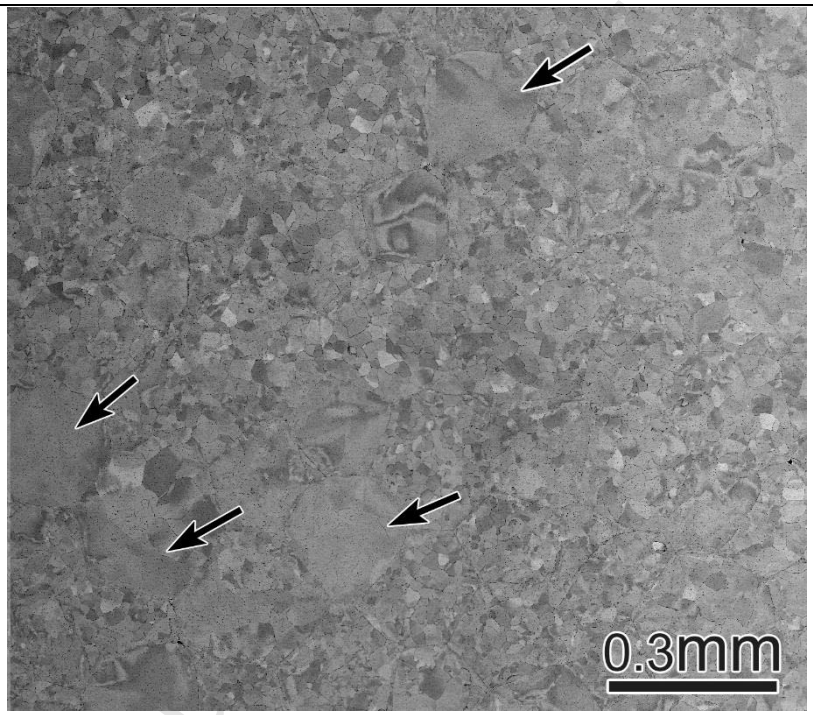

(a)

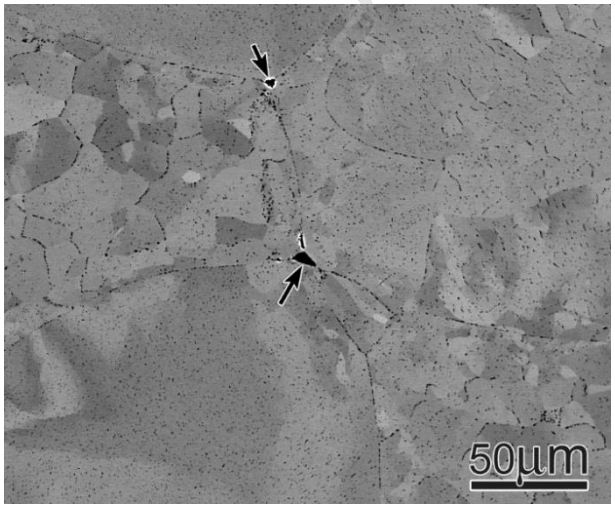

(b)

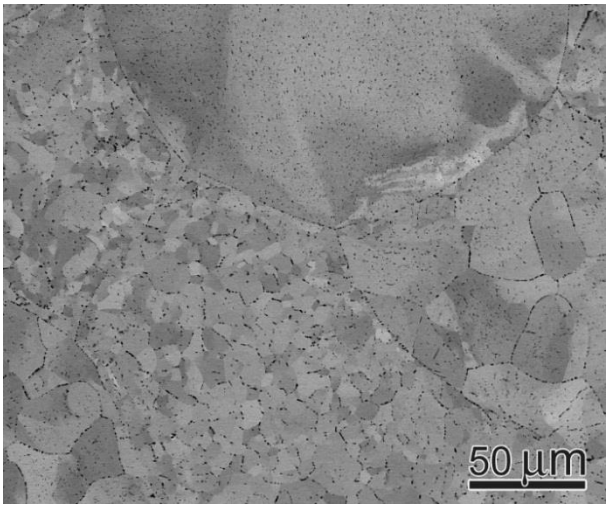

(c)

Figure 2 SEM images obtained from the sample HIPped at 900°C, showing some pores (arrowed) at triple junctions (b) and non-uniform grains (c). Note: Prior particles are arrowed

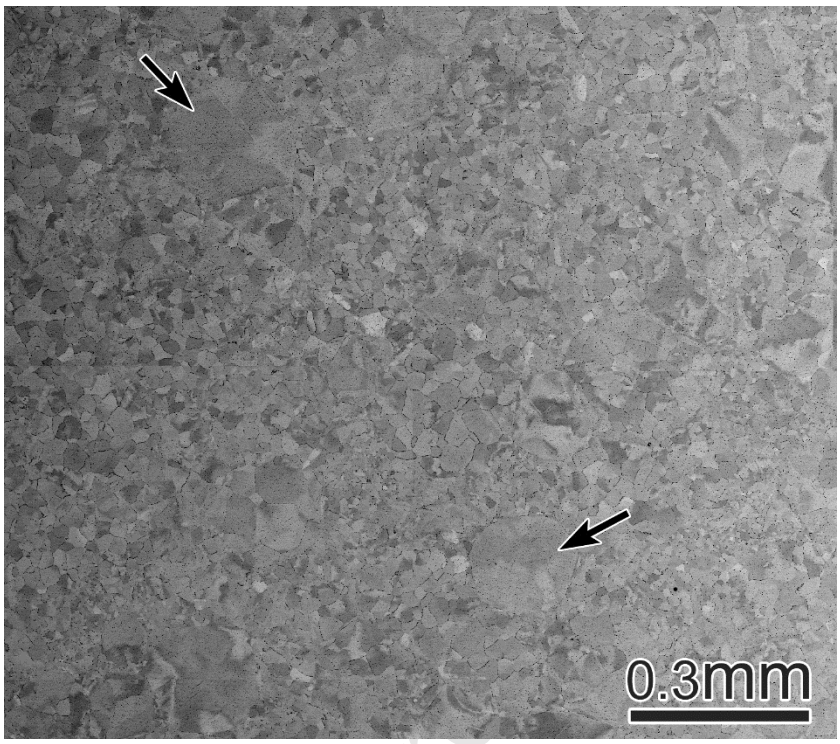

(a)

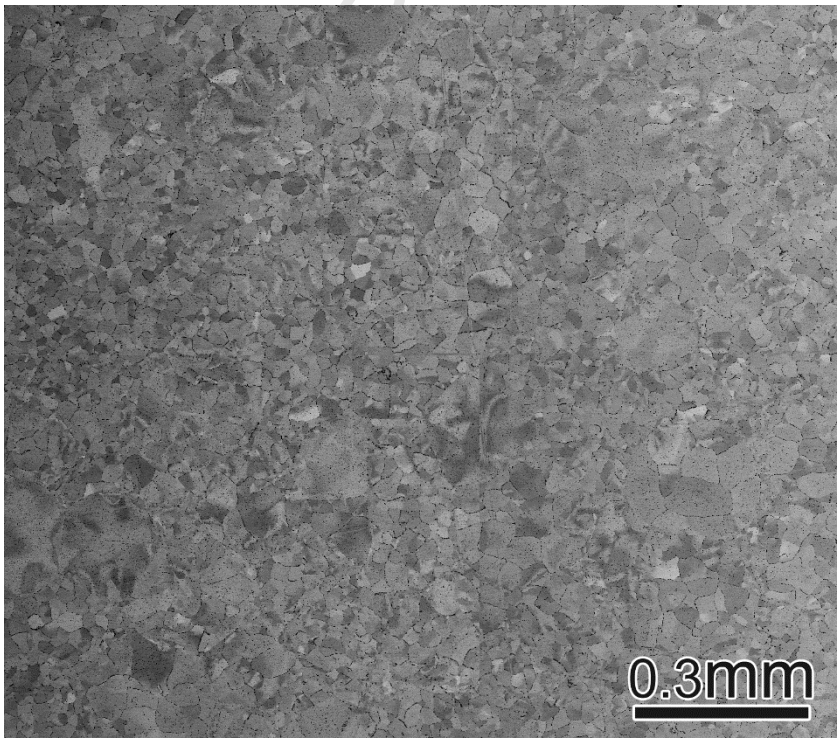

(b)

Figure 3 SEM images obtained from the sample HIPped at 950°C (a) and 980°C (b), showing that the amount of large grains in the sample HIPped at 980°C is lower than that in the sample HIPped at 950°C. Note: Prior particles are arrowed in Fig. 3a.

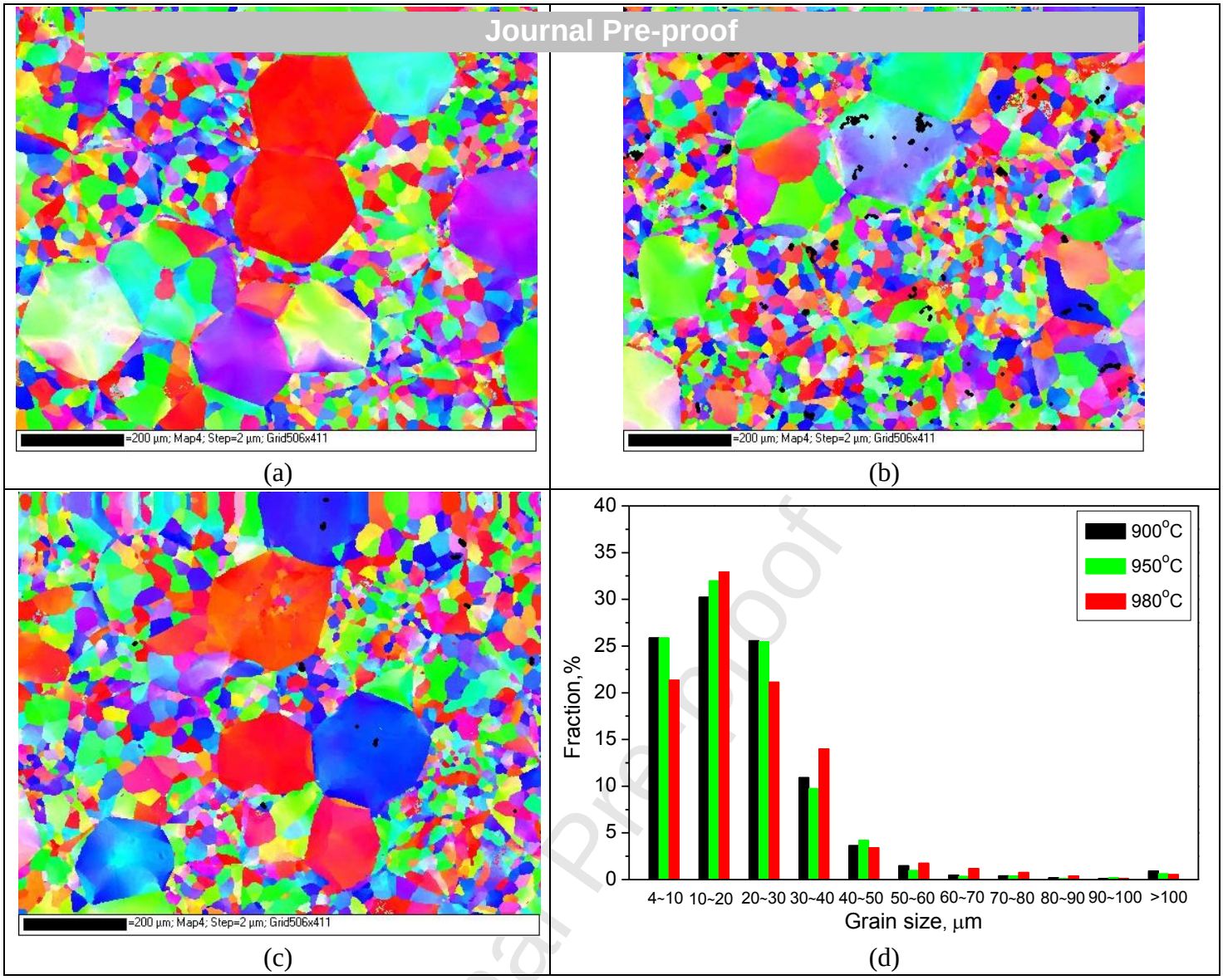

Figure 4 Inverse Pole Figure (IPF) EBSD maps of the samples HIPped at 900°C (a), 950°C (b) and 980°C (c), and the distribution of grain size of those three samples (d). (For interpretation of the references to colour in this figure legend, the reader is referred to the web version of this article.)

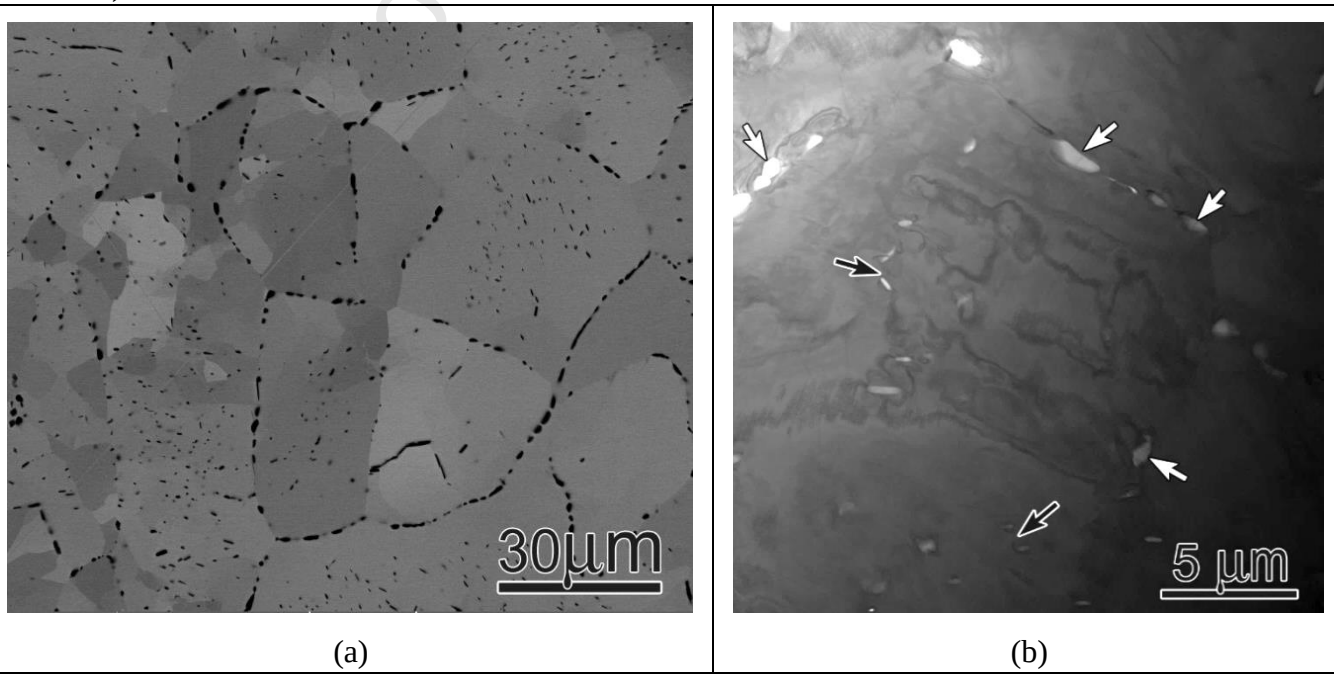

Figure 5 SEM (a) and bright field (BF) STEM (b) images of the sample HIPped at 950°C, showing that the size of carbide at grain boundaries is larger than that in the grain interior.

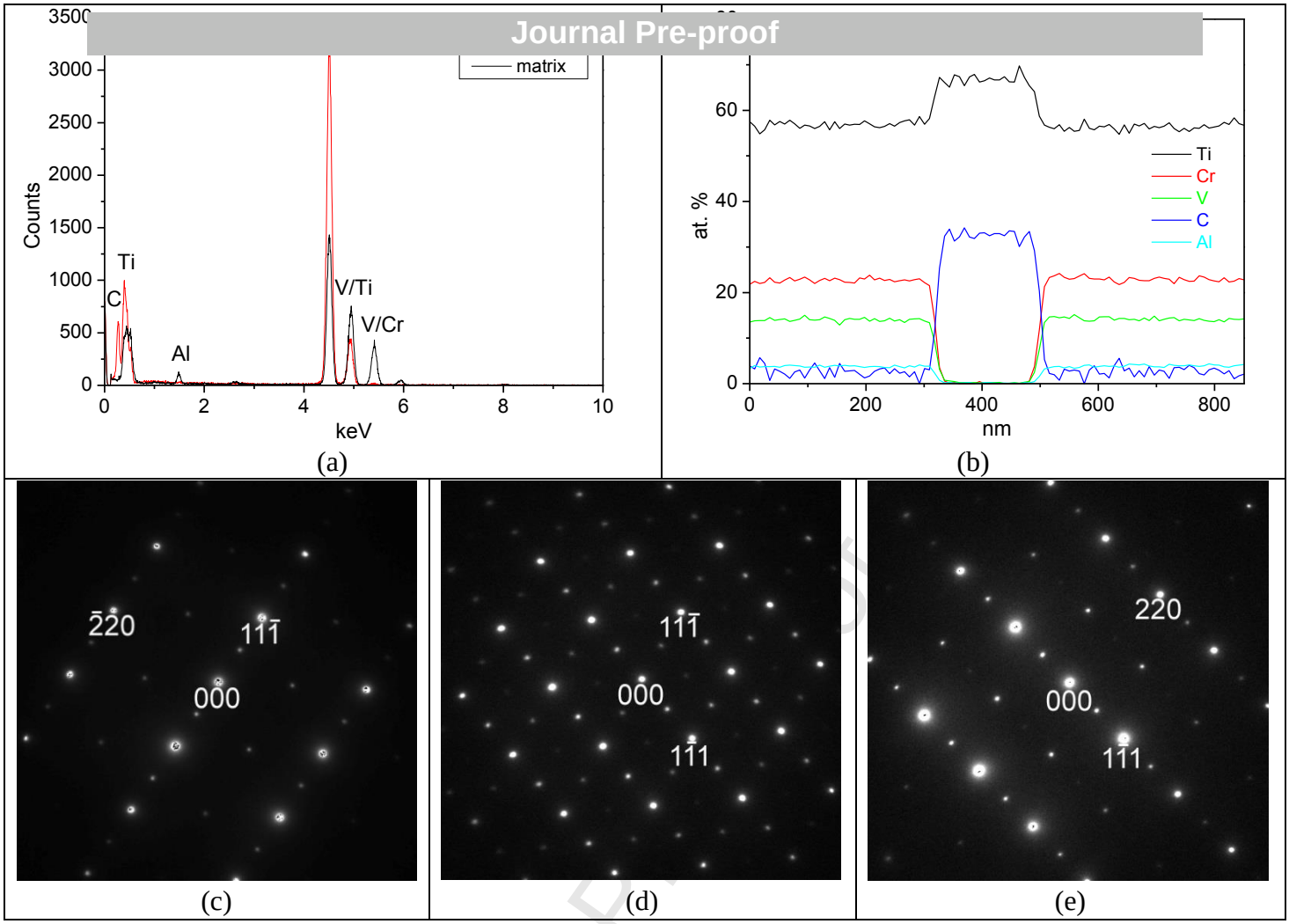

Figure 6 Spot EDS spectra from a carbide and matrix (a), EDS linescan across a carbide (b), and SAEDs were recorded along [112] (c), [011] (d) and [$\bar{1}$12] (e) from a carbide.

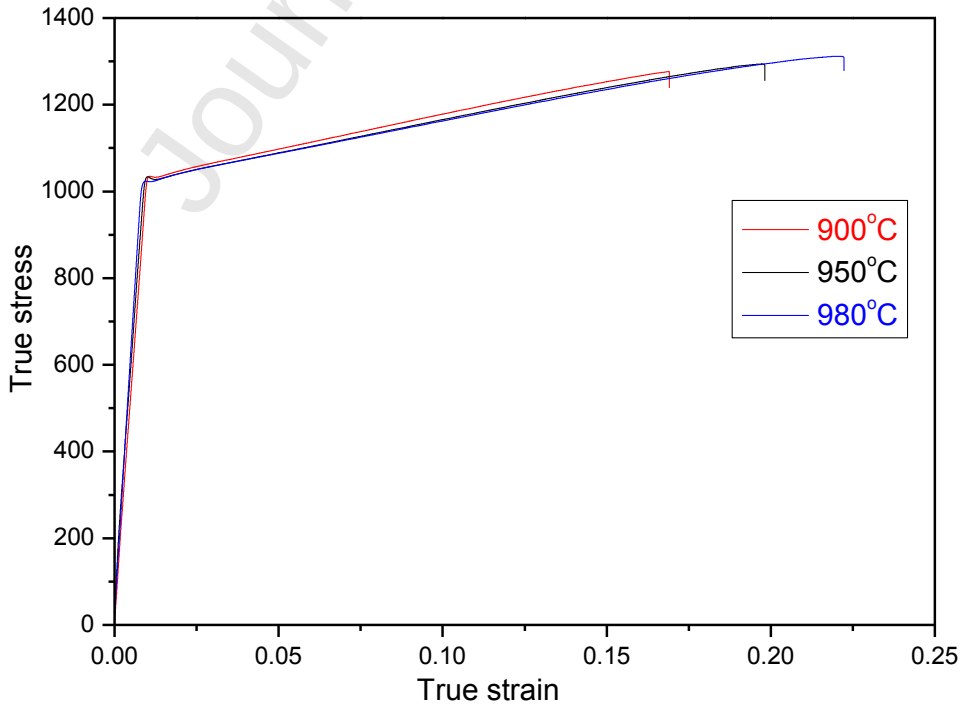

Figure 7 Typical stress-strain curves for the samples HIPped at 900, 950, and 980 °C.

Table 1 Summary of the tensile properties of powder HIPped Ti-25V-15Cr-2Al-0.2C alloy with different conditions and data from literature.

Samples	YS (MPa)	UTS (MPa)	Ductility (%)
HIPped at 900°C, 200MPa, 2h (this study)	1028 ± 7	1223 ± 111***	16/17/21
HIPped at 950°C, 200MPa, 2h (this study)	1028 ± 4	1271 ± 50	20/22/14
HIPped at 980°C, 200MPa, 2h (this study)	1022 ± 3	1300 ± 23	24/22/24
HIPped at 900°C, 100MPa, 2h*	972 ± 7	1040 ± 5	25/24/18
HIPped at 900°C, 100MPa, 4h*	996 ± 3	1044 ± 5	9/8/7
HIPped at 950°C, 150MPa, 2h*	997 ± 1	1057 ± 13	25/17/15
Extrued*	924 ± 13	964 ± 9	26/19/27
Forged Ti30V15Cr0.2Si**	1010	1020	21.5
Forged Ti20V15Cr0.2Si**	1005	1010	21.5
Forged Ti25V10Cr0.2Si**	910	930	23

Note: * - the same alloy as this study [11], ** - from [19], and *** - large error bar caused by low UTS for a sample.

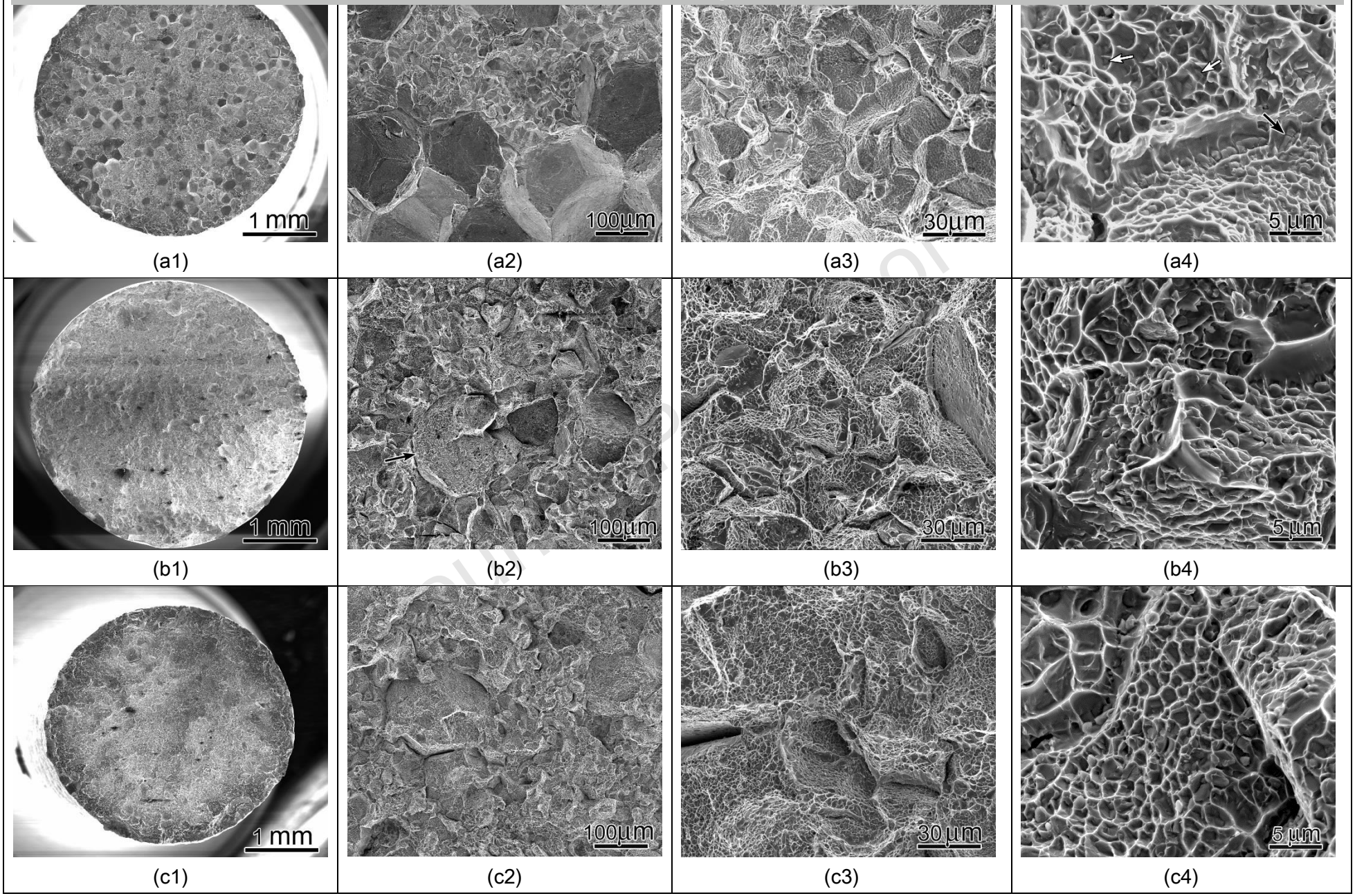

Figure 8 Fractography analysis on fracture surfaces of the tensile failed samples HIPped at (a) 900°C, (b) 950°C, and (c) 980°C at low (1) and high (2-4) magnification.

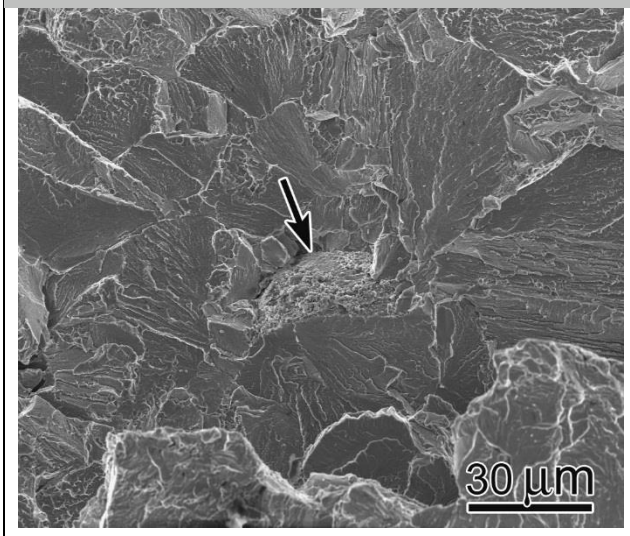

(a)

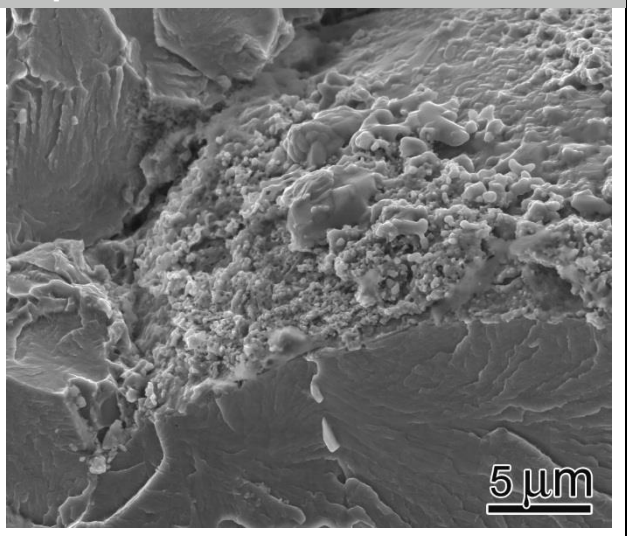

(b)

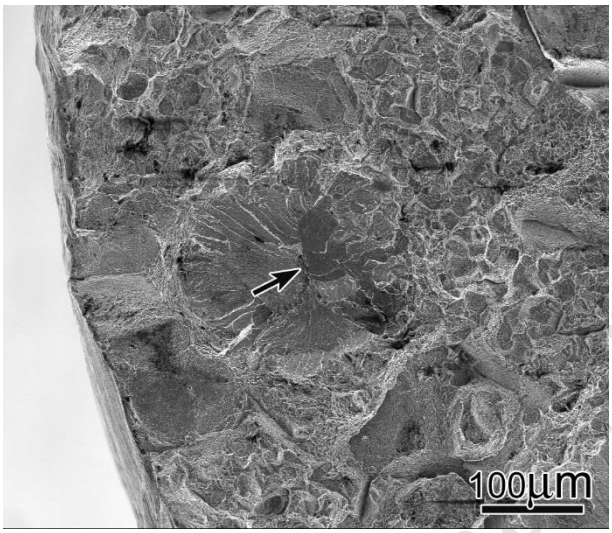

(c)

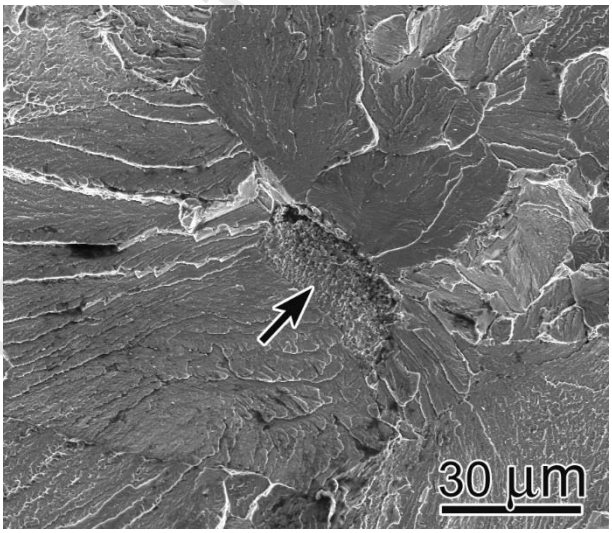

(d)

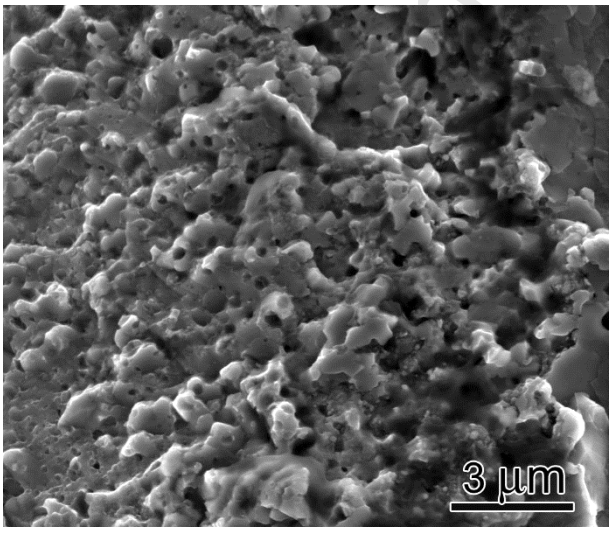

(e)

Figure 9 A SEM image of the fracture surface of the tensile sample with low ductility (i.e. 14%) showing a crack initiation site (arrowed) (a), high magnification of (a) (b); SEM images of fracture surface of the tensile sample with low ductility (i.e. 16%) and UTS (1096 MPa) showing that cracking initiation site (arrowed) (c) located likely at trip grain junctions (d), and high magnification of the

initiation site (e) exhibiting that bonding is not complete.

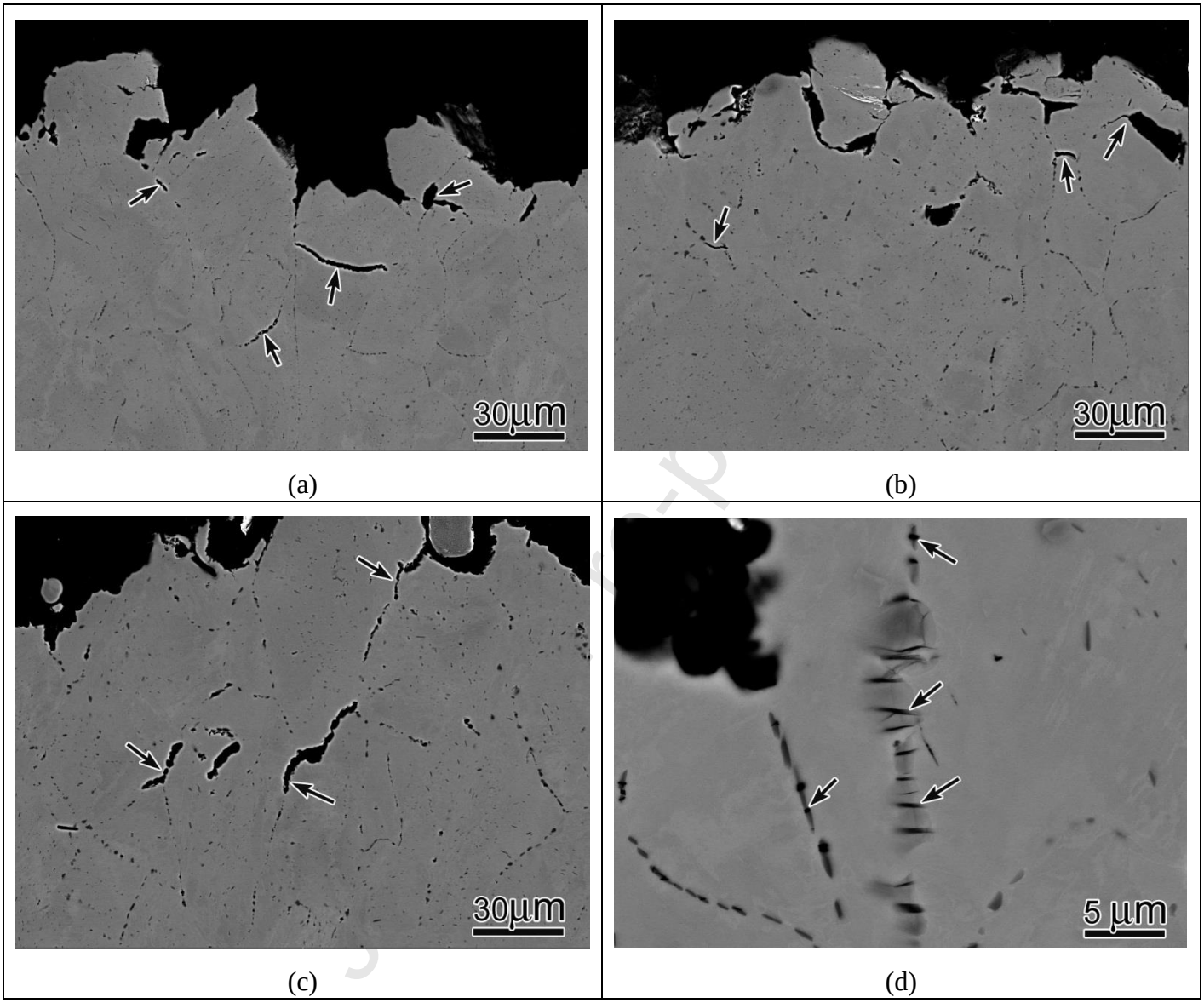

Figure 10 SEM images of the longitudinal cross-sectioned samples HIPped at 900°C (a), 950°C (b), and 980°C (c), showing cracking associated with the grain boundaries (arrowed), and the carbides broken (arrowed) (d).

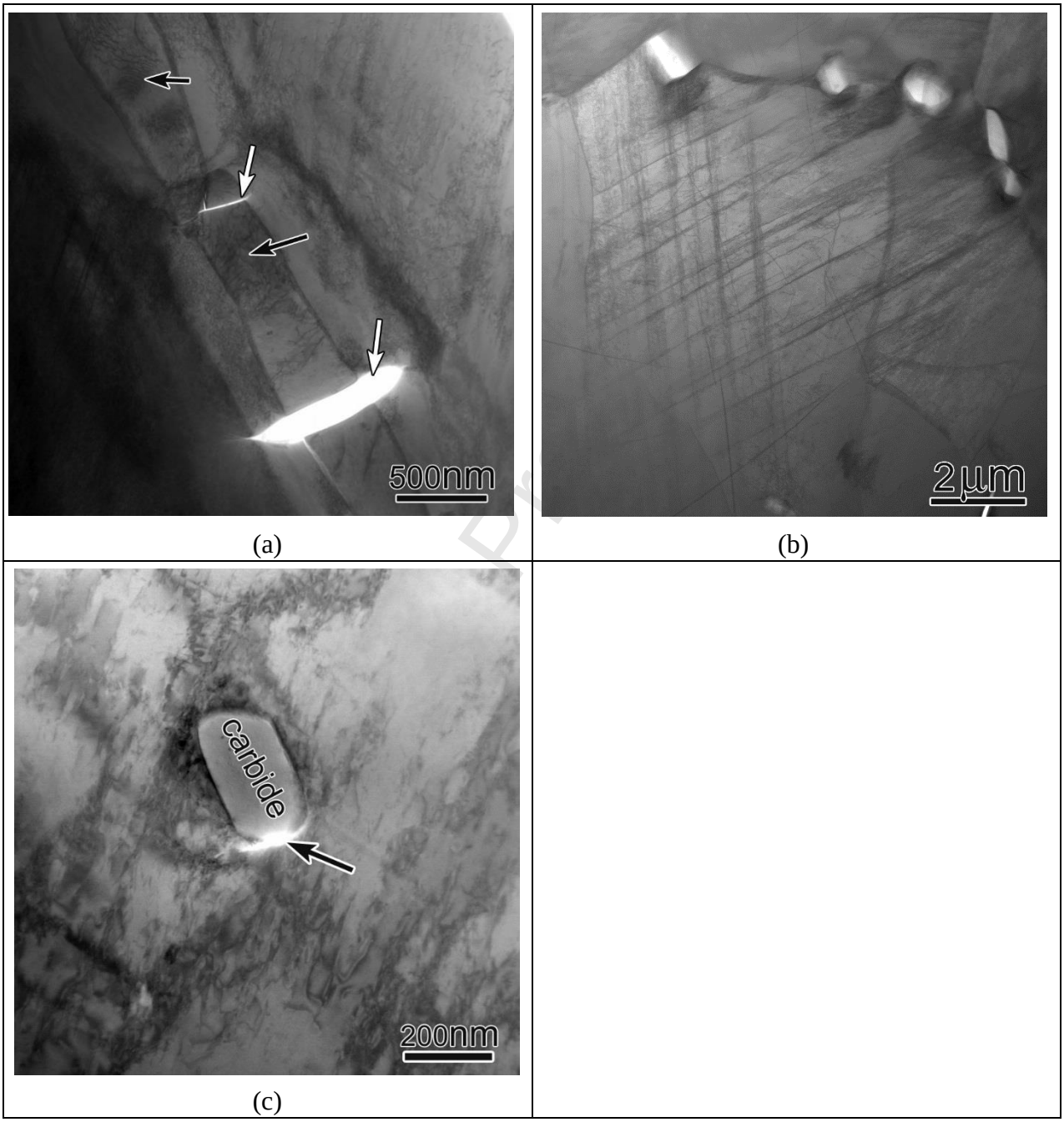

(a) (b) (c)

Figure 11 Multi-beam STEM images taken from the failed sample HIPped at 950°C. Some dislocations in the carbides (black arrows) and the carbide broken (white arrows) (a), slip bands and higher density of dislocations in the regions close to the carbides (white phases) (b), and cracking at interface of the carbide and matrix (arrowed)(c).

Highlights

5. A burn-resistant Ti25V15Cr2Al0.2C alloy was fabricated by HIPping at 900, 950, and 980°C for 2 h.
6. Some porosities were observed at triple-junctions of the HIPped sample at 900°C, leading to low ductility.
7. HIPping at 980°C produces the best tensile properties with over 20% ductility.
8. The carbide is an ordered fcc structure Ti_2C.